

E. ARICI¹,
H. HOPPE¹
F. SCHÄFFLER²
D. MEISSNER³
M.A. MALIK⁴
N.S. SARICIFTCI¹

Morphology effects in nanocrystalline CuInSe₂-conjugated polymer hybrid systems

¹ Linz Institute for Organic Solar Cells (LIOS), Physical Chemistry, Johannes Kepler University Linz, Altenberger Str. 69, 4040 Linz, Austria
² Semiconductor Physics, Johannes Kepler University Linz, Altenberger Str. 69, 4040 Linz, Austria
³ Fachhochschule Wels, Roseggerstr. 12, 4600 Wels, Austria
⁴ Department of Chemistry, Manchester University, Oxford Road, Manchester M13 9PL, UK

Received: 25 July 2003/Accepted: 9 December 2003
Published online: 5 March 2004 • © Springer-Verlag 2004

ABSTRACT We investigated blends of poly hexylthiophene (P3HT) with copper indium diselenide nanocrystals for photovoltaic applications. Depending on the synthesis, the particles were shielded by different organic surfactants. Different concentrations of these nanoparticles were suspended in the polymer solutions and spin cast onto ITO glass. Morphological studies have been performed by atomic force microscopy and transmission electron microscopy. Films consisting of tri-*n*-octylphosphine oxide-capped CISE : P3HT show photovoltaic response. The best performance we obtained is an open-circuit voltage of about 1 V and a photocurrent of 0.3 mA/cm² using a white light illumination intensity of 80 mW/cm².

PACS 78.66.Sq

1 Introduction

The high absorption coefficient, low band gap of about 1.0 eV and radiation stability make CuInSe₂ (CISE) a promising material for light harvesting. CISE have been prepared using molecular beam epitaxy [1, 2], liquid-phase epitaxy [3] and halogen vapour epitaxy [4]. High efficiencies for CISE solar cells were obtained by vacuum co-evaporation methods [5–7], but using these methods is rather difficult due to the variations of the stoichiometry on the large film area.

It has been shown recently that CISE nanoparticles can act as electron acceptors when mixed with *p*-type conjugated polymers. *n*-type CuInSe₂ (and also CuInS₂/*p*-type polypyrrole (PPy)) heterojunctions were prepared using electrochemical techniques [8]. The studies showed that the deposition of a thin PPy film onto CuInS₂ (CIS) is preferable for the device fabrication. Using bilayer device configurations of ITO/CIS/PPy/Ag an open-circuit voltage of about 0.5 V and a short-circuit current of 6.5 mA/cm² have been observed under illumination of 100-mW/cm² intensity.

Herein we report a solution-processed preparation of CISE and conjugated polymer thin-film layers, which can be used as photoactive layers. An advantage of blending inorganic nanoparticles with polymers in organic solvents is to

form large-area films by low cost processing techniques like spin casting. These techniques permit easy control of the layer thickness. A large variety of organic compounds, small molecules or polymers allows the fabrication of different cell designs such as single-layer or multilayer configurations using this technique.

The basic principles of hybrid solar cells are similar to the bulk heterojunction concept utilised by *p*-type conjugated polymers and *n*-type C₆₀ derivatives [9, 10]. Replacing the flat interface by an interconnected network structure of *p*- and *n*-type materials leads to a high surface area in the whole volume for charge separation, i.e. the 'bulk heterojunction'. In bulk heterojunction cells, the transport of the carriers to the electrodes without recombination is a more complicated problem to solve. An effective transport requires that, once the electrons and holes are separated onto different materials, each carrier type has a pathway to the appropriate electrode without needing to pass through a region of the other material. For an effective charge separation in electron donor/acceptor composites, the average distance between formed excitons in one material and the other material should be in the exciton-diffusion range of the polymers, which determines the size of domains.

For a profitable morphology of the blends, nanoscale inorganic particles should be used. To give an idea, the fullerene molecules embedded in the polymer are < 1 nm in diameter approximately; the cluster size, however, is heavily dependent on the processing conditions. It has been shown that composite films cast from toluene solutions result in much bigger (50–500-nm scale) fullerene clusters as compared to chlorobenzene-cast films with much finer grain sizes (below 50 nm) [11, 12].

Our first studies on hybrid solar cells were based on quantised CIS nanoparticles embedded in highly *p*-doped polymers. Due to the size quantisation effect, the band gap was larger than that of the macroscopic CIS. A hypsochromic absorbance shift up to 300 nm has been reported in acetonitrile dispersions [13]. Also, the matrix polymer poly(3,4-ethylene-dioxythiophene)/poly(styrenesulfonate) is a weak absorbing material.

In this contribution, we report CISE nanoparticles which may be small enough for profitable morphologies but do not show size quantisation effects. The CISE particles investigated have an absorbance edge at about 1000 nm [14]. These par-

ticles were mixed with regioregular poly(3-hexylthiophene) (P3HT), which is an effective hole-transport material in its regioregular form, with field effect hole mobilities up to $0.1 \text{ cm}^2 \text{ V}^{-1} \text{ s}^{-1}$ [15]. P3HT has the advantage that it absorbs in the visible range and may contribute to the charge creation in the bulk [16].

The first requirement in inorganic/organic hybrid solar cells is to blend a high concentration of inorganic nanoparticles into the polymer matrix to form a percolated network. Phase separation on the macroscopic scale should be avoided.

We investigated CISE nanoclusters capped with organic ligands. The organic shell can alter the dispersion characteristic of the inorganic particle by initiating attractive forces with the polymer chains, in which the particles should be homogeneously arranged. On the other hand, the van der Waals interaction between the CISE core and the organic shell should be strong enough to avoid the desorption of the organic ligand in film-preparation conditions. Therefore, we followed two different synthesis routes which lead to CISE nanoparticles with different surfactants. High-resolution transmission electron microscope (HRTEM) images of the CISE particles synthesised using the decomposition method revealed a narrow distribution of the particle sizes of about 15–20 nm. The shape of the investigated nanoparticles were mostly sharp-edged, rather than spherical [14]. On the other hand, whisker-like shapes have been obtained using a solvothermal route [17, 18]. The morphological properties of the polymer–CISE blend films have been observed by atomic force microscopy (AFM) and scanning electron microscopy (SEM) measurements. Current–voltage measurements have been performed on heterostructures, where ITO and Al contacts have been used as anode and cathode, respectively.

2 Experimental

2.1 Materials

The materials investigated are shown in Fig. 1. Poly hexylthiophene (P3HT) is commercially available from Aldrich. Synthesis of CuInSe_2 particles has been performed by using a hot injection method [14, 19]. Se, tri-*n*-octylphosphine (TOP), tri-*n*-octylphosphine oxide (TOPO), indium (III) chloride and Cu(I) iodide were purchased from Aldrich. TOPO and TOP were purified by vacuum distillation at 250°C . TOP is the liquid phase similar in nature to the surfactant TOPO.

The synthesis of the TOPO-capped CuInSe_2 nanoparticles has been reported elsewhere in more detail [14]. Briefly, a stoichiometric dispersion of InCl_3 and CuI has been prepared in a TOP–TOPO mixture. At high temperatures (330°C), a stoichiometric amount of tri-*n*-octylphosphine selenide was injected into the reaction mixture. Thereby, a spontaneous colour change from yellow to black occurs. TOPO, which is a polar coordinating Lewis base, is in an excess amount in the mixture. After cooling the solution to 80°C , the nanoparticles were washed three times with methanol to remove any excess TOPO and other organic impurities and resuspended in toluene for further investigations. The product was black in colour.

We also synthesised ethylenediamine-capped CISE by a solvothermal route described by Qian et al. [20–22]. A stoi-

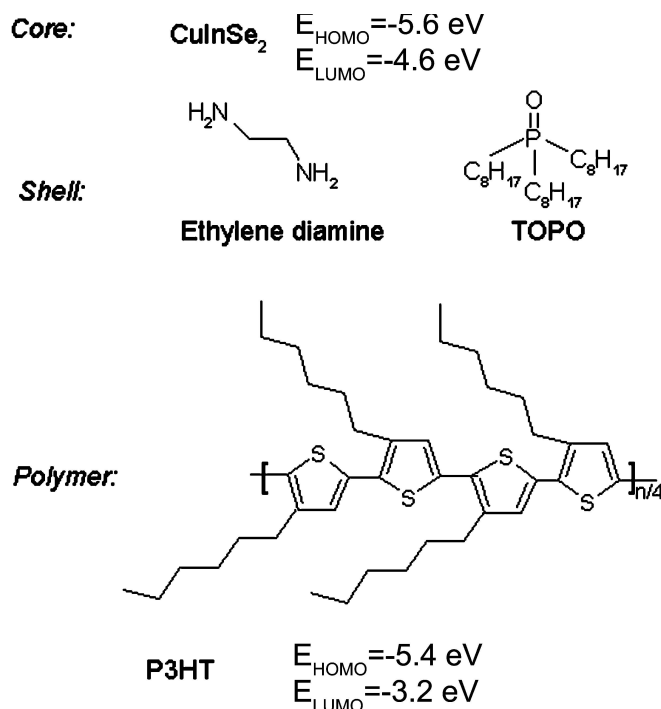


FIGURE 1 Chemical structures of the materials investigated

chiometric mixture of elementary Se, $\text{CuCl}_2 \times 2\text{H}_2\text{O}$ and $\text{InCl}_3 \times 4\text{H}_2\text{O}$ was loaded into a 50-ml autoclave, which was then filled with anhydrous ethylenediamine up to 80% of the total volume. The experiment was performed at 180°C for 15 h. The product was washed with water and ethanol several times in order to remove the by-products. The product was black in colour, which predicts the non-quantised nature of the particle.

2.2 Cell preparation and experimental methods

Blends of CISE and P3HT were prepared from a ~ 3 wt. % toluene solution by spin casting onto ITO glass (supplied by BALZER) in air. Film thicknesses in the order of 200 ± 30 nm were obtained in this way. The films were annealed at 150°C under vacuum for 2 h. The morphology of the films has been studied by AFM. Aluminium (300 nm) was evaporated as a counter electrode on the films.

The size of the prepared CISE nanoparticles was studied by transmission electron microscopy on a Jeol 2012 FasTEM at 200 kV.

The crystallographic structure of the products was determined by powder X-ray diffraction (XRD) using $\text{Cu } K_\alpha$ radiation of 1.5418 \AA . The scan rate of 0.1° s^{-1} was applied to record the patterns in the 2θ range of $10\text{--}60^\circ$.

Current–voltage (I – V) measurements were performed at room temperature in argon environment using a Keithley 617 source-monitor unit. For electrical characterisation the cells were illuminated with 80-mW/cm^2 power intensity of white light by a Steuernagel solar simulator. The active area was about 5 mm^2 . The filling factor FF was calculated by $FF = V_p \times I_p / (V_{oc} \times I_{sc})$ with V_p and I_p being the voltage and current of the maximum power point and V_{oc} and I_{sc}

the open-circuit voltage and the short-circuit photocurrent, respectively.

3 Results and discussion

3.1 Material properties of the CISE nanoparticles

3.1.1 X-ray investigations. The XRD patterns of CuInSe₂ nanoparticles are shown in Fig. 2.

An intense peak at $2\theta = 27.0^\circ$ oriented along the (112) direction and other prominent peaks observed at 44.6° ((220)/(204)) and 52.7° ((312)/(116)) identify the chalcopyrite structure of CuInSe₂ prepared by the thermal decomposition method (Fig. 2, sample A). These patterns are in good agreement with JCPDS data [23]. Additionally, weak orientations at 30.9° , 51.1° and 60.9° are observed, which may occur due to the existence of by-products Cu₂Se and In₂O₃.

In the range between 15 and 35° a broad halo appears, probably due to an amorphous contribution. This may indicate that TOPO is still present, which may not have been removed completely.

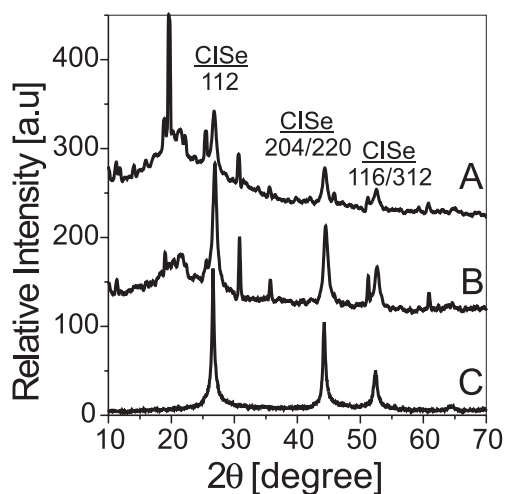


FIGURE 2 X-ray-diffraction patterns of CISE nanocrystals with different sample histories shown in arbitrary units. Sample A and sample B were synthesised using the decomposition method. Sample A has been washed in MeOH for 10 min to remove the organic surfactants (sample B for 40 min). Sample C was synthesised using the solvothermal route

In order to remove the excess amount of TOPO and the by-products, the nanocrystals were washed for 30 min with methanol and resuspended in toluene. During the washing process, including centrifuging afterwards, most of the by-products have been partly removed, which can be concluded from the X-ray data (Fig. 2, sample B). The intensity of the by-product peaks for sample B is lower than for the case of sample A.

The plot C shows the results of X-ray-diffraction investigations performed on the CISE prepared by the solvothermal route. The three reflections at 2θ values of 27.9° (112), 46.5° ((220)/(204)) and 55.0° ((312)/(116)) are those of the chalcopyrite structure of CISE (Fig. 2, sample C). In contrast to samples A and B, there is no amorphous contribution.

3.1.2 TEM investigations. High-resolution transmission electron microscope (HRTEM) images of the TOPO-capped CISE particles revealed a distribution of the particle sizes of about 15–20 nm. The shape of the investigated nanoparticles was mostly sharp-edged (Fig. 3b). As the concentration of the nanocrystals increased, a broad diffraction pattern could result from the overlap of many nanoparticles with different orientations (Fig. 3a). In concentrated CISE layers, the resolution of the TEM images is limited because of the overlapping of the differently oriented nanoparticles. However, the shape and size of the CISE-capped nanoparticles do not change.

Synthesis of CISE following the solvothermal route leads to elongated particles. CISE samples prepared using concentrated CISE dispersions show whisker-shaped particles with dimensions of at least 20 nm (Fig. 4a). High resolution transmission electron microscopy (HRTEM) together with electron diffraction (ED) was used on diluted CISE dispersions to provide information about crystallinity (Fig. 4b).

Recent observations of the relationship between the particle shape and the solvent made for the solvothermal synthesis of CISE as well as PbS nanoclusters showed that ethylenediamine can act as a bidentate ligand [20–22]. This could facilitate the formation of chelate complexes of $[\text{Cu}(\text{en})_2]^+$ and likely forcing the CuInSe₂ grains to grow in one direction. We also observed a tendency for elongated particles using

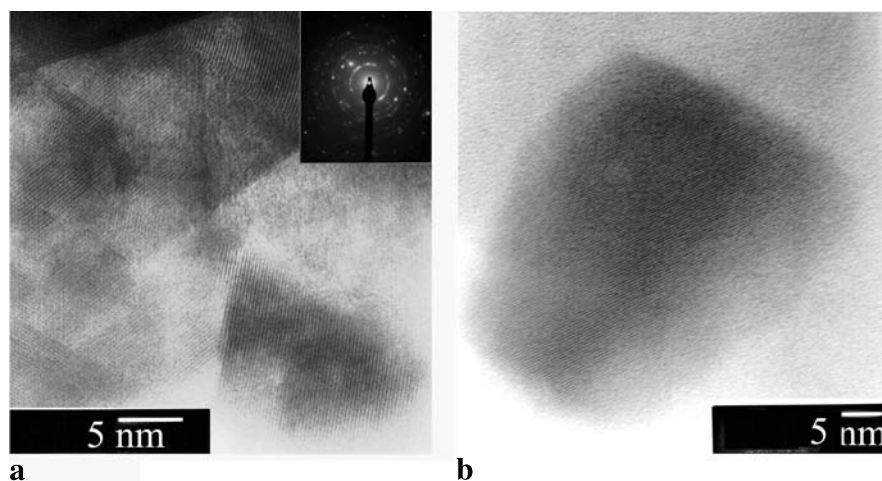


FIGURE 3 HRTEM images of TOPO-shielded CISE particles. **a** From concentrated, **b** from diluted nanoparticle dispersions. The selected-area electron-diffraction pattern of the nanoparticles shows the presence of polycrystalline nanostructures with the characteristic broad reflections

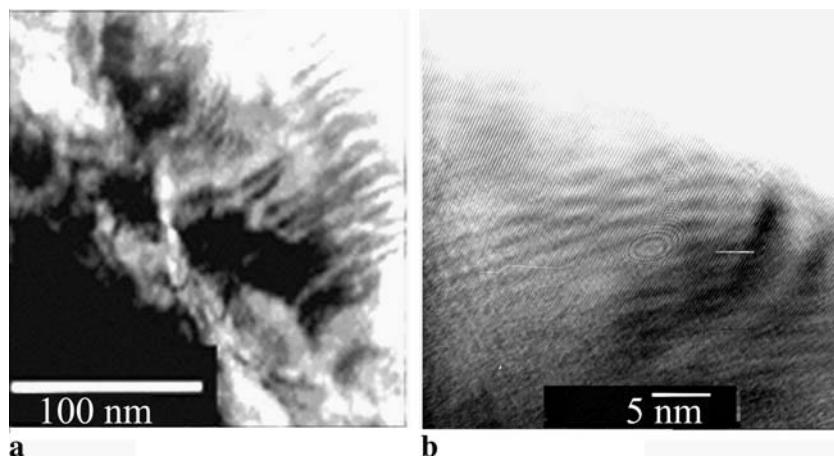


FIGURE 4 **a** TEM images of ethylenediamine-shielded CISE particles from concentrated dispersions show elongated particles with dimensions of above 20 nm. **b** HRTEM images from diluted CISE dispersions were used to determine the crystallinity

the solvothermal method; on the other hand, a major limitation seems the aggregation of the particles in concentrated dispersions.

Inductively coupled plasma atomic emission spectroscopy (ICPAES) analysis (Cu, In, Se) of the nanoparticles shows the stoichiometry to be $\text{Cu}_1\text{In}_1\text{Se}_2$ using the solvothermal route as well as the decomposition route (not shown here).

3.2 Material properties of the CuInSe_2 -P3HT blends

3.2.1 AFM-SEM investigations. To study the effect of chemical nature and amount of the surfactant on the morphology of the CISE : P3HT blends, atomic force microscopy (AFM) and scanning electron microscopy (SEM) measurements have been carried out. Films in a weight ratio of CISE : P3HT = 10 : 1 were prepared by using CISE, with different sample histories as described in Sect. 3.1.1. Films have been annealed at 150 °C for 2 h under vacuum.

According to the X-ray investigations, shown in Fig. 2, sample A, CISE, which has been washed in methanol for a shorter time, has a higher amount of the surfactant. We prepared two films via spin coating using toluene dispersions of a 10 : 1 wt.% CISE : P3HT (90 wt. % CISE) mixture, whereas the surfactant amount of the CISE was varied first (Fig. 5a and b). In comparison, the morphology of CISE nanoparticles

shielded with ethylenediamine has been investigated by SEM (Fig. 5c).

In general, the interaction between the polymer chains and the TOPO-capped CISE nanoparticle is attractive enough to avoid a large-scale phase separation. On the other hand, using TOPO-rich samples leads to film morphologies that consist of big pinholes with a diameter of about 0.5 μm , which are probably formed during the annealing process due to the removal of excess TOPO and toluene (Fig. 5a). Consequently, the photovoltaic devices prepared from these layers were influenced by an ohmic contribution (not shown here).

CISE that has been washed in methanol for 30 min longer consists of less TOPO considered by the weak amorphous contribution to the X-ray diffractogram in Fig. 2. The topology of the P3HT blends prepared using the TOPO-‘poor’ CISE reveals a smooth surface with a roughness of about 50 nm and a homogenous morphology (Fig. 5b). The films are almost pinhole-free. Accordingly, for the photovoltaic characterisation, films have been characterised only by using a thoroughly washed CISE sample.

In contrast to the TOPO-capped CISE, the morphology of the blends of P3HT and ethylenediamine-capped CISE particles is characterised by large-scale phase separation (Fig. 5c). SEM investigations of these blends show islands of CISE clusters with a diameter of several micrometres. Desorp-

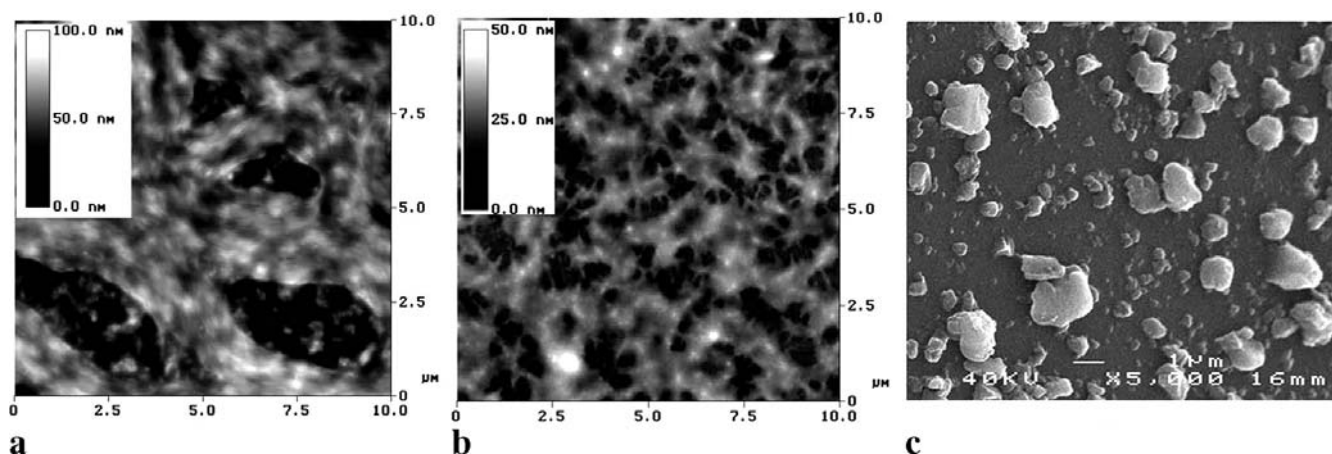


FIGURE 5 AFM images of blends consisting of CISE : P₃HT in a weight ratio of 10 : 1 depending on the CISE preparation (see also Fig. 2). **a** TOPO-rich CISE, **b** TOPO-poor CISE and **c** ethylenediamine-capped CISE in P₃HT matrices

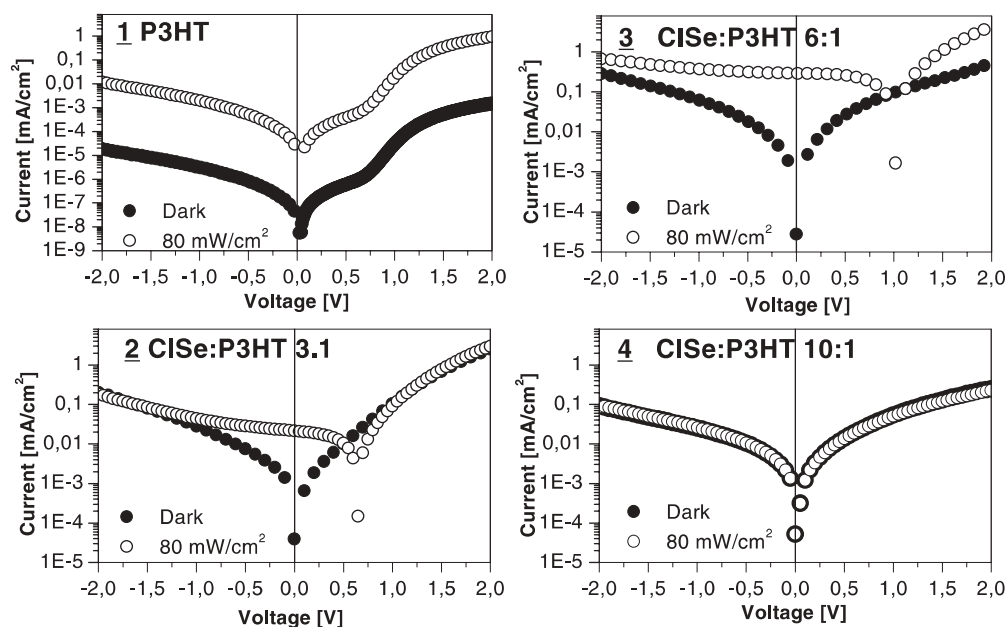


FIGURE 6 I - V characteristics of P3HT/CISe (TOPO-poor) hybrid devices with increasing CISe amount in comparison to pure P3HT devices in the dark and under AM 1.5 illumination (semi-logarithmic plots)

tion of ethylenediamine during the film preparation leads to an aggregation of the inorganic nanoparticles and therefore to a non-profitable morphology. No photovoltaic effect could be determined using these CISe particles.

3.2.2 Diode characteristics. In polymer/nanocrystal blends, when the nanocrystal surface is coated with a thicker TOPO layer, we find no photovoltaic response. The studies performed on CISe blends, which have been washed in methanol for 30 min longer, show a photovoltaic effect, which depends on the CISe ratio (in wt.%).

Typical current-voltage (I - V) curves for CISe-P3HT blends are shown in Fig. 6. The I - V characteristics of the diodes have been obtained under argon with an irradiance of 80 mW/cm² through the ITO side.

In the case of a negative applied bias, i.e. positive contact to the Al and negative contact to the ITO, the purely P3HT devices delivered typically a rectification ratio in the dark of 77 at ± 2 V and 92 under illumination. Even though the polythiophene is known to exhibit a photovoltaic effect [24], there was no detectable photovoltaic effect using our preparation conditions (Fig. 6(1)). This observation should be partly due to the fact that the open-circuit voltage equal to 28 mV is low compared to the theoretical upper limit, which is the difference between the work functions of the two electrodes. The limit is estimated to be 0.4 V for an ITO/Al system.

Blends of CISe/P3HT have been prepared by varying the amount of the CISe in the films. By white-light illumination of an ITO/CISe-P3HT/Al cell (CISe : P3HT = 3 : 1) with a power intensity of 80 mW/cm², we received open-circuit voltages V_{oc} of 0.65–0.70 V and short-circuit current densities I_{sc} of 20–30 μ A/cm² (Fig. 6(2)). The calculated fill factor of the diode is 0.42. The rectification ratio in the dark is 12 at ± 2 V and 16 under illumination.

A remarkable approach to enhance the photovoltaic properties was using blends of CISe-P3HT in a weight ratio of 6 : 1 in the same cell design. These devices delivered a short-circuit current of 0.3 mA/cm² and an open-circuit voltage of 1 V.

From sample to sample, there were differences for the I_{sc} values in a range of 0.2–0.3 mA and for the V_{oc} values in a range of 0.75–1 V. Existence of non-uniformly distributed surfactant areas on the surface can lead to contact problems, which is not easy to control. The rectification ratio in the dark is 7 at ± 2 V and 5.3 under illumination. The calculated fill factor of the diode is 0.5.

Enhancing the CISe amount in the polymer to a weight ratio of 10 : 1 in the same cell design results in a decrease of the rectification ratios to 2.6 in the dark at ± 2 V and 2.75 under illumination. There was no detectable photovoltaic effect (Fig. 6(4)).

Hybrid materials are three-component systems including the surfactant TOPO, which is an isolator. Increasing the CISe concentrations in the polymer matrix also leads to an enhancement of the surfactant amount in the sample. When the concentration of the surfactant is above a critical value, the electro-optical interaction between the polymer and nanoparticles might be suppressed (Fig. 6(4)). A comparison between Fig. 6(2), 6(3) and 6(4) shows systematically the increase of the series resistance of the diode by increasing the amount of TOPO-capped CISe. In the dark, the influence of the series resistance can be seen in the forward direction; the curves become flat and the injection currents are lower. Accordingly, the rectification ratios become lower.

The origin of the photovoltaic activity on CISe-P3HT blends has not been studied systematically until now. As a next step, we will further investigate photophysics of CISe-P3HT blends to distinguish between the electron- and energy-transfer processes, which are possible driving forces for the photovoltaic activity.

4 Conclusions

Hybrid organic-inorganic photovoltaic junctions based on CISe nanoparticles have been investigated. Their main advantage should be their potential for a low-cost, large-

area fabrication. Blends of CISE and P3HT have been prepared from solution via spin coating. The influence of the surfactant on the morphology has been determined by AFM and SEM investigations. Films consisting of TOPO-capped CISE : P3HT in a weight ratio of 6 : 1 show a significantly better photovoltaic response in comparison to a P3HT single layer. A further increase of the nanoparticle amount, on the other hand, leads to the breakdown of the diode behaviour. Enhancement of the cell performance can be accomplished by improving the nanocrystal–polymer interface to remove the surface traps. A good balance between the three components should be defined experimentally, to fulfil the requirements for an effective hybrid cell.

ACKNOWLEDGEMENTS This work is sponsored by the Deutsche Bundesministerium für Bildung und Forschung, Förderkennzeichen 01SF0026. We express our sincere thanks to P. Skabara, Inorganic Chemistry, Manchester University, UK.

REFERENCES

- 1 V.K. Kapur, M. Fischer, R. Roe: *Mater. Res. Soc. Symp. Proc.* **6**, 668 (2001)
- 2 H.W. Schock, U. Rau: *Physica B* **1081**, 308 (2002)
- 3 M.E. Beck, M. Cocivera: *Thin Solid Films* **71**, 272 (1996)
- 4 T. Negami, Y. Hoshimoto, M. Nishitani, T. Wada: *Sol. Energy Mater. Sol. Cells* **49**, 343 (1997)
- 5 M.A. Contreras, B. Egaas, K. Ramanathan, J. Hiltner, A. Swartzlander, F. Hasoon, R. Noufi: *Prog. Photovolt.* **7**, 311 (1999)
- 6 K. Kushiya: *Thin Solid Films* **387**, 257 (2001)
- 7 V.K. Kapur, A. Bansal, P. Le, O.I. Asensio: *Thin Solid Films* **431** textbfupto432, 53 (2003)
- 8 S. Bereznev, J. Kois, E. Mellikov, A. Öpik, D. Meissner: 'CuInSe₂/ Polypyrrrole Photovoltaic Structure Prepared by Electro-deposition'. Presented at: *17th Eur. Photovoltaic Solar Energy Conf., Munich, Germany, 22–26 October 2001*
- 9 S. Shaheen, C.J. Brabec, F. Padinger, T. Fromherz, J.C. Hummelen, N.S. Sariciftci: *Appl. Phys. Lett.* **78**, 841 (2001)
- 10 C.J. Brabec, F. Padinger, J.C. Hummelen, R.A.J. Janssen, N.S. Sariciftci: *Synth. Met.* **102**, 861 (1999)
- 11 C.J. Brabec, N.S. Sariciftci, J.C. Hummelen: *Adv. Funct. Mater.* **1**, 15 (2001)
- 12 T. Munters, T. Martens, L. Goris, V. Vrints, J. Manca, L. Lutsen, W. de Ceuninck, D. Vanderzande, L. De Schepper, J. Gelan, N.S. Sariciftci, C.J. Brabec: *Thin Solid Films* **403–404**, 247 (2002)
- 13 E. Arici, N.S. Sariciftci, D. Meissner: *Adv. Funct. Mater.* **13**, 165 (2003)
- 14 E. Arici, H. Hoppe, D. Meissner, F. Schäffler, A. Malik, N.S. Sariciftci: *Thin Solid Films*, in press
- 15 H. Sirringhaus, N. Tessler, R.H. Friend: *Science* **280**, 1741 (1998)
- 16 F. Padinger, R.S. Rittberger, N.S. Sariciftci: *Adv. Mater.* **13**, 1 (2003)
- 17 B. Li, Y. Xie, J. Huang, Y. Qian: *Adv. Mater.* **11**, 1456 (1999)
- 18 E. Arici, H. Hoppe, A. Reuning, N.S. Sariciftci, D. Meissner: 'CIS Plastic Solar Cells'. Presented at: *17th Eur. Photovoltaic Solar Energy Conf., Munich, Germany, 22–26 October 2001*
- 19 M.A. Malik, N. Revaprasadu, P. O'Brien: *Adv. Mater.* **11**, 1441 (1999)
- 20 Y. Qian: *Adv. Mater.* **11**, 1101 (1999)
- 21 Y. Xie, Y. Qian, W. Wang, S. Zhang, Y. Zhang: *Science* **272**, 1926 (1996)
- 22 B. Li, Y. Xie, J. Huang, Y. Qian: *Adv. Mater.* **11**, 1456 (1999)
- 23 H.L. Hwang, C.L. Cheng, L.M. Liu, Y.C. Liu, C.Y. Sun: *Thin Solid Films* **67**, 83 (1980)
- 24 J.J. Dittmer, E.A. Marsaglia, R.H. Friend: *Adv. Mater.* **12**, 1270 (2000)